Journal of Ceramic Processing Research. Vol. 17, No. 4, pp. 313~317 (2016)

J O U R N A L O F
Ceramic Processing Research

Lightweight corundum-mullite refractories: II, Effects of porous aggregates on the slag resistances of corundum-mullite refractories

Wen Yan*, Qingjie Chen, Xiaoli Lin, Junfeng Chen and Nan Li
The State Key Laboratory of Refractories and Metallurgy, Wuhan University of Science and Technology, Wuhan, China

Corrosion of five corundum-mullite refractories with the different porous aggregates and the same matrix by the blast furnace slag was conducted using the static crucible test. Effects of properties of corundum-mullite aggregates on the slag resistance of refractories were investigated through X-ray diffractometer (XRD), scanning electron microscopy (SEM), and mercury porosimetry measurement, etc. It is found that the porous corundum-mullite aggregates have different slag absorbing capacity, which affects the composition of the corroded aggregates and matrices at slag/refractory interface, and thus affects the slag corrosion and penetration resistances. Comparing with the dense corundum-mullite refractory, the porous corundum-mullite aggregate with 31.6% apparent porosity (AP) substituting the dense aggregates in the refractories does not make the slag resistance degenerate and reduces the bulk density by 16.7 wt%; whereas, when the APs of aggregates increase to 41.6-44.8%, the slag resistance sharply deceases. It is a successful case that the developed lightweight refractory with high slag resistance has a potential application for working lining of high-temperature furnace.

Key words: Lightweight corundum-mullite refractories, Porous aggregates, Slag resistance, Pore characteristics, Phase compositions.

Introduction

With increased demand for saving energy in high temperature industries, more attention has been devoted to the researches on the heat-insulating refractories [1-7]. Heat-insulating refractories closest to the hot face have better heat insulation function [8]. However, traditional lightweight refractories can't be used as working lining in high-temperature furnace due to their low slag resistance [1, 9]. So, it is necessary to develop lightweight refractories with high slag resistance to be used as working linings of high-temperature furnace.

Dense corundum-mullite refractories have been widely used as working lining in high-temperature furnace because of their high mechanical strength, excellent corrosion resistance, high heat and creep resistance at high temperature, and so on [10-14]. Usually, dense aggregates are used to prepare corundum-mullite refractories. Actually, the aggregates with high density and low porosity may not be necessary, because the matrix is more easily to be corroded by slag [1, 15]. If the porous aggregates have high slag resistance similar with the matrices, the refractories would have enough slag resistance to be used as working lining of high-temperature furnace, including the slag working lining [1, 15].

In our another work [16], the effects of pore characteristics and phase compositions on the slag resistance of the porous aggregates were investigated, and found that with an increase in apparent porosities (1.4-41.6%), the slag penetration and corrosion resistances of aggregates decrease evidently. However, when the dense corundum-mullite aggregates were substituted by the porous in the refractories, the change of the slag resistance of the refractories has not been understood. It will be addressed in the present work.

*Corresponding author:
Tel : +86-027-68862511
Fax: +86-027-68862121
E-mail: yanwen@wust.edu.cn

Experimental Procedure

Five corundum-mullite refractories were fabricated using the same matrix and different porous aggregates, including rectangle parallelepiped samples with the size of 140 mm length × 25 mm width × 25 mm thickness for the porosity and density measurement and XRD analysis, and cylindrical blocks in which there is a hole with a diameter of 23 mm and a depth of 18 mm for the slag resistance testing. Their matrix consists of 71.5 wt% mullite powder (70 wt% Al_2O_3, Guangming Refractory Technologies Co. Ltd., China) and 28.5 wt% corundum powder (99.7 wt% Al_2O_3, Zili Refractory Technologies Co. Ltd., China). Their aggregates have the same particle size distribution and volume percentage in refractories. These aggregates are DCMA, PCMA1, PCMA2, PCMA3 and PCMA4 in the other work [16], their apparent porosities (APs), bulk densities (BDs), average pore sizes (APZs) and relative phase contents are listed in Table 1. The five refractories in the present work are referred as CDCMA, CPCMA1, CPCMA2,

Table 1. Apparent porosities, bulk densities, average pore sizes and relative phase contents (wt%) of aggregates [16].

	DCMA	PCMA1	PCMA2	PCMA3	PCMA4
Apparent porosity (%)	1.4	31.6	41.6	42.3	44.8
Bulk density (g/cm^3)	3.18	2.28	1.96	1.94	1.86
Average pore size (im)	1.40	3.41	3.16	2.74	5.64
Corundum	28	31	32	39	34
Mullite	72	69	68	61	66

Table 2. Chemical compositions of the aggregate, matrix and the slag (wt%).

	SiO_2	Al_2O_3	Fe_2O_3	CaO	MgO	K_2O	Na_2O	Ti_2O	MnO
Aggregates	19.38	79.89	0.18	0.07	0.06	0.05	0.18	0.19	–
Matrix	16.01	79.34	1.20	0.48	0.39	0.15	0.03	2.40	0.00
Slag	31.50	16.08	0.75	40.17	9.92	–	–	0.81	0.40

CPCMA3 and CPCMA4 according to their different aggregates. After the specimens heated at 1500 ºC for 3 h, the cylindrical blocks filled with 16 g slag were heated at 1550 ºC for 3 h in air, and then furnace-cooled. The chemical compositions of the aggregate, matrix and the slag are listed in Table 2.

After corrosion testing, crucibles were cross-sectioned perpendicularly to the slag-refractory interface, as shown in Fig. 1. The actual corroded and penetrated areas in each specimen were measured by counting pixels method. Corrosion here is defined as regions of refractory completely replaced by slag. The corrosion index IC and penetration index IP are obtained by following equation: $I_C(_P) = S_C(_P) / S_O$; S_O is the original section area of the crucible inner chamber; S_C is the section area of refractory completely replaced by slag; S_P is the penetrated section area.

The APs and BDs were detected by Archimedes' principle using water as the medium. The phase transformation were characterized by X-ray diffractometry (XRD, Philips Xpert TMP). The pore size distribution (PSD) and APZ were measured through mercury porosimetry measurement (AutoPore IV 9500, Micromeritics Instrument Corporation). Microstructures of these samples were observed by a field emission scanning electron microscope (FESEM, Nova 400 NanoSEM, FEI Company, USA) equipped with energy dispersive X-ray spectroscope (EDS, INCA IE 350 Penta FET X-3, Oxford, UK). Compositions of predicated phases were calculated from Equilibrium mode by the FactSage® 6.2 thermochemical software based on the EDS results.

Results and Discussion

The apparent porosities (APs) and bulk densities (BDs) of specimens containing different aggregates are shown in Fig. 2. For the specimen CDCMA containing the dense aggregate with 1.4% AP, the AP is 24.0%, the BD is 2.57 g/cm^3. When the AP of the aggregate increases to 31.6%, the AP of specimen CPCMA1 is 34.9%, and the BD is 2.14 g/cm^3. With the increase of the APs of aggregates to 41.6-44.8%, the APs of specimens CPCMA2, CPCMA3 and CPCMA4 are 37.7-39.6%, and the BDs are 1.99-2.05 g/cm^3.

The corrosion and penetration indexes of the five corroded specimens are shown in Fig. 3. Comparing with the dense CDCMA, the specimen CPCMA1 has a better performance in penetration and corrosion resistances because of its lower corrosion and penetration indexes. Whereas, when the AP of aggregates increase to 41.6-44.8%, especially for CPCMA3 and CPCMA4, the penetration index increases greatly and the corrosion

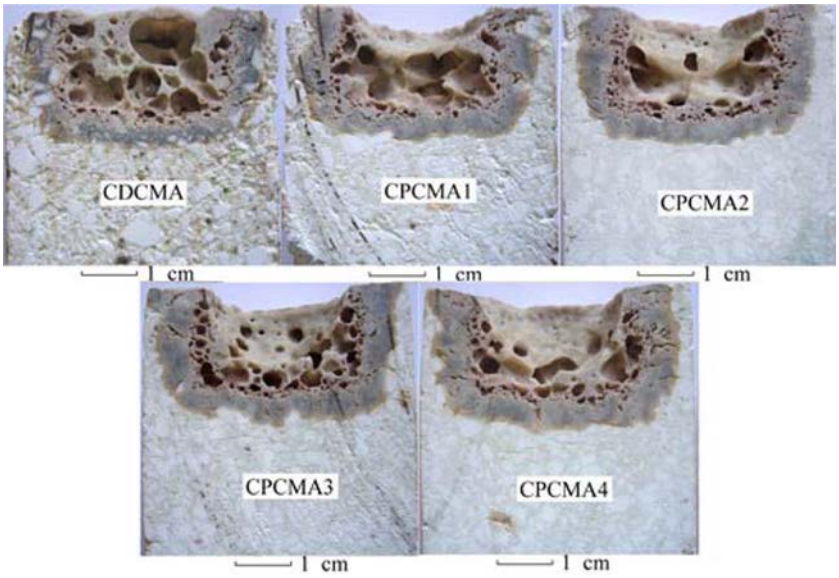

Fig. 1. Photographs of the specimens after the slag tests (vertical cut).

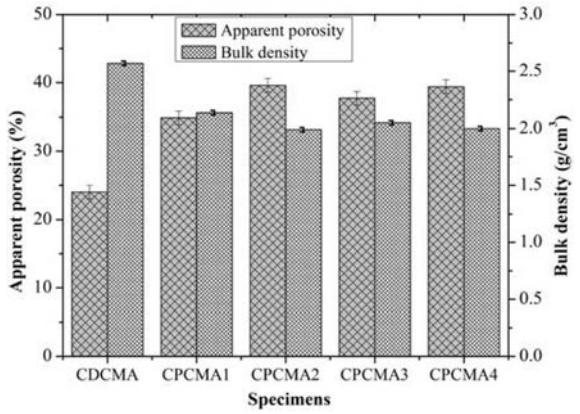

Fig. 2. Apparent porosities and bulk densities of the specimens containing different aggregates.

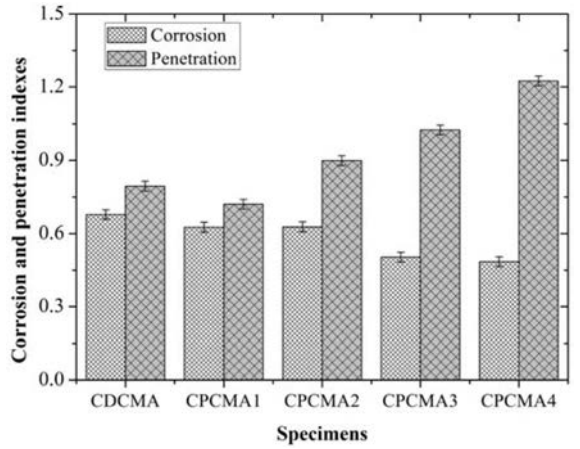

Fig. 3. Corrosion and penetration indexes of the specimens corroded for 3h at 1550 ºC.

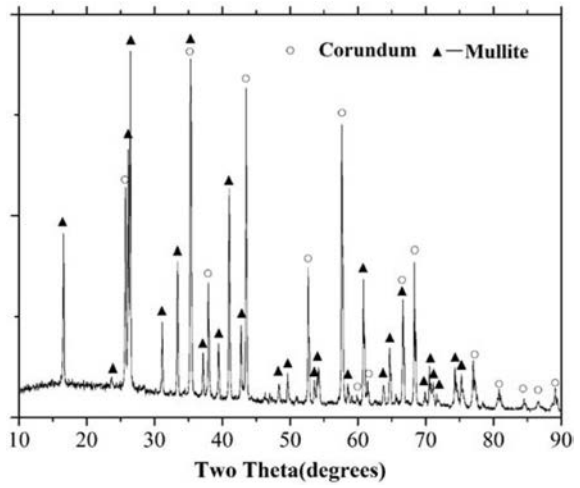

Fig. 4. XRD pattern of the matrix.

index increases evidently. However, it doesn't means that the three specimens perform better in corrosion resistance, which would be discussed in the later.

Obviously, a conclusion could be drawn based on the above testing results: the dense corundum-mullite aggregates substituted by the porous with 31.6% AP in the refractories

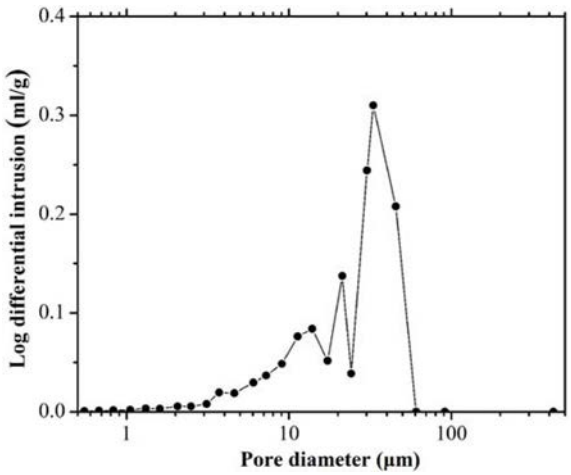

Fig. 5. Pore size distribution of the matrix.

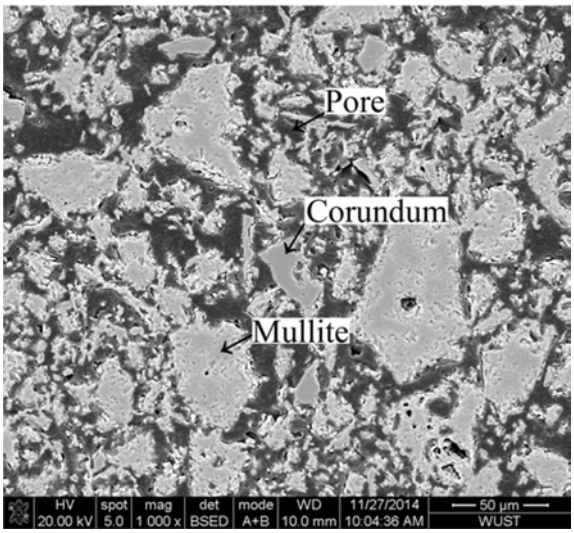

Fig. 6. Microstructure of the matrix.

does not make the slag resistance degenerate, and reduces the BD by 16.7 wt%. To understand the effects of porous aggregates on the slag resistances of lightweight corundum-mullite refractories, two issues need to be considered.

One issue is the difference in the phase compositions and microstructures of the five aggregates and the matrices, which would affect the slag penetration and the dissolution of refractory into slag. The five refractories have the matrices with the same phase composition, pore size distribution (PSD) and microstructure, as shown in Figs. 4-6. The matrix consists of 71 wt% mullite and 29 wt% corundum. In the other work [16], it's found that the higher the corundum content, the higher the corrosion resistance is. So, only considering the phase composition, the matrix has the similar corrosion resistance with the aggregate DCMA, but has the lower corrosion resistance than the aggregates PCMA1-PCMA4. Additionally, the matrix has a larger average pore size (APZ) of 31.37 mm, which is almost 10-17 times than those of the aggregates, and thus the

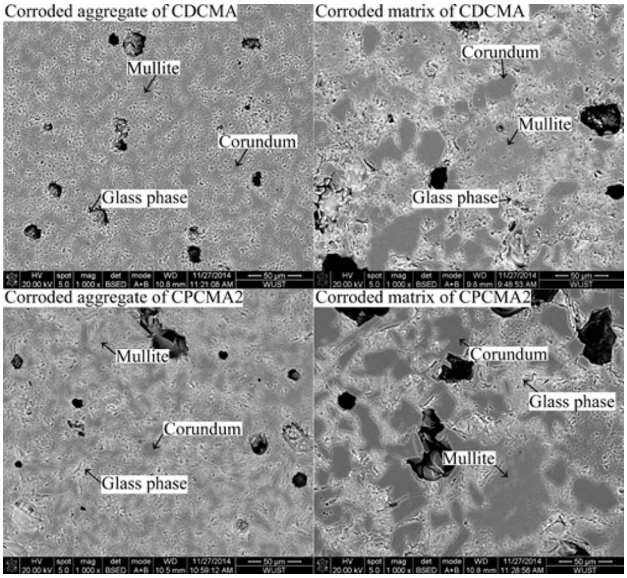

Fig. 7. Microstructures of the corroded aggregates and matrices at the slag/refractory interfaces of CDCMA and CPCMA2.

penetration resistance of the matrix is obviously lower than those of the aggregates.

The other issue that needs to be considered is the slag absorbing capacity of the five types of aggregates, which would affect the reaction between the matrix and the slag, and then change the compositions of the corroded aggregates and matrices at high temperature. To understand the changes in the slag absorbing capacity of all the aggregates clearly, the microstructures of the corroded aggregates and matrices at the slag/refractory interfaces of the five specimens were observed in the experiment. Fig. 7 shows the microstructures of the corroded aggregates and matrices at the slag/refractory interfaces of CDCMA and CPCMA2. In the corroded aggregate and matrix of CDCMA, the fuscous contrast phases are mullite and corundum, and the white contrast phase are glass phase. With an increase of the AP of aggregate, the corundum content of the corroded aggregate decreases, whereas the corundum content of the corroded matrix increases. It means that the slag absorbing capacities of the five types of aggregates are rather different, which strongly affects the compositions of the corroded matrices.

The EDS results of the corroded aggregates and matrices are listed in Tables 3 and 4, respectively. The corroded aggregates consist of Al_2O_3, SiO_2, CaO and minor TiO_2, and the corroded matrices consist of Al_2O_3, SiO_2, CaO, and minor TiO_2, Na_2O and MgO. Based on the EDS results, the phase compositions of the corroded aggregates and matrices and the viscosities of the slag were calculated through the FactSage® package at the thermodynamic equilibrium condition (1550 °C), also listed in Tables 3 and 4. For the dense CDCMA, the corroded aggregate consists of 46.16 wt% corundum, 38.19 wt% mullite and 15.65 wt% slag, and the viscosity of the slag is 1.682 Pa · S; the corroded matrix consists of 64.07 wt% mullite and 35.93 wt% slag, and the viscosity of the slag is 2.079 Pa · S. For the CPCMA1, in the corroded aggregate, no corundum exists, the contents of mullite and slag increase, and the viscosity of the slag increases to 34.284 Pa · S; whereas, in the corroded matrix, the contents of mullite and corundum increase, the content of slag decrease, and the viscosity of the slag decreases to 1.683 Pa · S. With a further increase of AP of aggregate, the contents of slag in the corroded

Table 3. EDS results of the corroded aggregates at the slag/refractory interfaces of specimens and their phase composition and viscosity of slag at 1550 °C.

	EDS results (wt%)				Phase composition (wt%)			Viscosity
	Al_2O_3	SiO_2	CaO	TiO_2	Corundum	Mullite	Slag	(Pa · S)
CDCMA	81.37	15.90	2.73	0.00	46.16	38.19	15.65	1.683
CPCMA1	61.78	35.13	3.09	0.00	0	74.04	25.96	34.284
CPCMA2	61.54	34.12	3.29	1.05	0	71.73	28.27	9.566
CPCMA3	58.13	38.11	3.76	0.00	0	67.54	32.46	39.809
CPCMA4	58.71	34.46	6.83	0.00	0	57.63	42.37	3.905

Table 4. EDS results of the corroded matrices at the slag/refractory interfaces of specimens and their phase composition and viscosity of slag at 1550 °C.

	EDS results (wt%)						Phase composition (wt%)			Viscosity
	Al_2O_3	SiO_2	CaO	TiO_2	Na_2O	MgO	Corundum	Mullite	Slag	(Pa · S)
CDCMA	61.60	32.01	3.67	1.65	1.07	0.00	0	64.07	35.93	2.079
CPCMA1	67.38	28.16	4.46	0.00	0.00	0.00	3.39	71.05	25.56	1.683
CPCMA2	66.30	26.94	6.76	0.00	0.00	0.00	16.01	45.25	38.74	1.683
CPCMA3	64.95	25.52	8.11	0.00	0.00	1.43	31.58	15.22	52.20	1.724
CPCMA4	62.65	25.79	9.63	0.00	0.00	1.92	36.36	0	63.64	1.662

aggregates and matrices increase. The difference between the results shown in Fig. 7 and those listed in Tables 3 and 4 indicates the reaction between the refractories and the penetrated slag has not finished in the experiment.

The higher apparent porosities and smaller pore size of the porous aggregates make them higher slag absorbing capacities than the matrix, which quickens the dissolution rate of the aggregates into the penetrated slag due to the higher capillary force caused from the smaller pore size. So, comparing with the matrix, the mullite and corundum in the porous aggregates more easily dissolve into slag, and make the penetrated slag rich in SiO_2 (Table 3), and then increase the viscosities of slag in the corroded aggregates. For the specimens CDCMA and CPCMA1, although the dense aggregate of CDCMA has the higher slag resistance because of the lower slag content (Table 3), the higher viscosities of the penetrated slag in the corroded aggregate and the less slag content in the corroded matrix of the specimen CPCMA1 make these two specimens have the similar slag resistance. Whereas, for the specimens CPCMA2, CPCMA3 and CPCMA4, their higher porosities make both the aggregates and matrices absorb more slag (Table 3, 4), which results in a sharp decrease in the corrosion and penetration resistances of these three specimens, although their corrosion indexes are relatively small (Fig. 3); additionally, the smallest pore size of the aggregate PCMA3 leads to the highest dissolution rate, and thus the viscosity of the penetrated slag is the highest in these three specimens.

If the porous aggregates apparent porosities and pore size distributions are properly controlled, it is visible that the slag resistances of the lightweight refractories do not decrease comparing with the dense counterparts when the dense corundum-mullite aggregates are substituted by the porous in the refractories.

Conclusions

(1) The higher apparent porosities and smaller pore size of the porous aggregates make them higher slag absorbing capacities than the matrix, which quickens the dissolution rate of the aggregates into the penetrated slag due to the higher capillary force caused from the smaller pore size. The slag absorbing capacity affects the composition of the corroded aggregates and matrices at slag/refractory interface, and thus affects the slag corrosion and penetration resistance.

(2) Comparing with the dense corundum-mullite refractory, the porous corundum-mullite aggregate with 31.6% AP substituting the dense aggregates in the refractories does not make the slag resistance degenerate and reduces the BD by 16.7 wt%; whereas, when the apparent porosities of aggregates increase to 41.6-44.8%, the slag resistance sharply decreases.

(3) It is a successful case that the developed lightweight refractory with high slag resistance has a potential application for working lining of high-temperature furnace.

Acknowledgments

The authors would like to thank the Educational Commission of Hubei Province of China (Grant No. Q20131111) and the Science Foundation of the State Key Laboratory of Refractories and Metallurgy of China (Grant No. 2014QN01) for financially supporting this work.

References

1. W. Yan, N. Li, Z. Miao, G.P. Liu and Y.Y. Li, J. Ceram. Process. Res. 13 (2012) 278-282.
2. W. Yan, N. Li, B.Q. Han, X.M. Fang and G.P. Liu, Ceram-Silikáty 54 (2010) 315-319.
3. W. Yan, N. Li, B. Q. Han, Am. Ceram. Soc. Bull. 84 (2005) 9201-9203.
4. W. Yan, N. Li, B.Q Han, J. Ceram. Process. Res. 11 (2010) 388-391.
5. W. Yan, N, Li, B. Han, Sci. Sinter. 41 (2009) 275-281.
6. R. Salomao, M.O.C.V. Boas, V.C. Pandolfelli, Ceram. Int. 37 (2011) 1393-1399.
7. W. Yan, N. Li, B. Han, Interceram: Refractories Manual (2009) 25-28.
8. N. Li, H. Gu, H. Zhao, in "Refractories Fundamental and Technology" (Metallurgical Industry Press, 2010) p. 9. (in Chinese).
9. M.N. Dunaeva, Refract. Ind. Ceram. 47 (2006) 199-200.
10. C. Aksel, Ceram. Int. 29 (2003) 183-188.
11. B. Meng, J.H. Peng, Ceram. Int. 39 (2013) 1525-1531.
12. J. Stjernberg, M.A. Olivas-Ogaz, M.L. Antti, J.C. Ion, B. Lindblom, Ceram. Int. 39 (2013) 791-800.
13. J.L. Liu, Refractories & Lime 34 (2009) 33-36, 40.
14. L.L Wang, Z.J. Li, J.L. Sun, D.Y. Zhang, X. M. Li, Ironmaking 20 (2001) 31-32 (in Chinese).
15. W. Yan, N. Li, B. Han, Int. J. Appl. Ceram. Technol. 5 (2008) 633-640.
16. W. Yan, X.L. Lin, J.F. Chen, Q.J. Chen, N. Li, J. Ceram. Process. Res. submitted.